Synthesis and Electrografting of Dendron Anchored OEGylated Surfaces and Their Protein Adsorption Resistance

Mary Jane L. Felipe, Ramakrishna R. Ponnapati, Roderick B. Pernites, Pampa Dutta, and Rigoberto C. Advincula*

Department of Chemistry and Department of Chemical and Biomolecular Engineering, University of Houston, Houston, Texas 77204-5003, United States

ABSTRACT In this study, a series of electrochemically active oligo(ethylene glycol) (OEG) linear-dendrons have been synthesized and grafted onto electrode surfaces by cyclic voltammetry (CV) to improve protein resistance. Dendronized molecules with peripheral carbazole functionality and branching architecture enabled tethering of the poly(ethylene glycol) (PEG) or OEG group with a predictable number of electrochemical reactive groups affecting OEG distribution and orientation. It is possible that ample spacing between the OEG chains affects the intrinsic hydration of these layers and thus surface protein resistance. The films were characterized by CV, surface plasmon resonance (SPR), static contact angle measurements, and atomic force microscopy (AFM). This approach should enable improved nonbiofouling properties on biorelevant electrode surfaces (metal or metal oxides) by potentiostatic or potentiodynamic electrochemical methods, providing an alternative to the self-assembled monolayer (SAM) approach for anchoring PEG layers.

KEYWORDS: electrografting • PEG • OEG • protein resistance • electrochemical • adsorption • SPR

The nonspecific adsorption of proteins to surfaces exposed to a physiological or biological environment usually leads to impaired surface biofunctionality, decreased receptor−ligand interaction, and denaturation of proteins (1−3). Mitigating this phenomenon is important for the nonbiofouling of metallic stents, guide wires and guiding catheters, and biosensors. A well-established strategy to minimize nonspecific adsorption of proteins is to coat the surface with poly(ethylene glycol) (PEG) or oligo(ethylene glycol) (OEG) (4−6). A variety of strategies for tailoring the surfaces of materials with OEG have been developed through the years leading to a better understanding of OEG's resistance to protein adsorption. Despite the extensive research, complete control of the short-term and long-term biofouling mechanism has not been realized. This is mainly due to the complexity of physiological processes in an in vivo biological milleu and the evolving mechanism of the biofouling process. Prime and Whitesides (1) showed that self-assembled monolayer (SAM)s presenting short oligomers of the ethylene glycol group ($n = 2-7$) are also highly effective in resisting the adsorption of proteins. Grunze et al. (6, 7) correlated the molecular conformation of oligo(ethylene glycol) (OEG)-terminated self-assembled alkanethiolate monolayers with the ability of these films to resist protein adsorption. They observed that dense and predominantly helical films of OEG-terminated SAMs are protein resistant. They have speculated that the conformational degree of solvation, and consequently the stability of an interfacial water layer, determines if the protein, reaching the surface by diffusion, can irreversibly adsorb onto the surface.

In this study, electrochemically active OEGylated linear-dendrons have been synthesized in order to use the electrochemical grafting method in modifying electrode surfaces for protein resistance (Figure 1). Because recent findings have shown that understanding water−OEG interaction is a vital step to examining the mechanism of protein resistance (8), the aim of this study is to provide an alternative approach based on electrochemical grafting in designing OEGylated surfaces that are usually fabricated through non-electrografting techniques like SAMs or adsorbed polyelectrolytes. In SAMs, the assembly of molecules on surfaces relies on their conformations allowing high degree of van der Waals interactions with the neighboring molecules leading to arrangements with secondary level of organization in the monolayer (7). In our system, the intra- and interchain connectivity among the carbazole dendron molecules determine the conformation of the individual OEG chains within the assembly including packing and ordering with respect to each other. Dendronized molecules are of high interest for their high peripheral functionality and branching architecture, providing a degree of control over reactivity and orientation. By tethering an OEG group on the focal point, the predictable shape and the number of reactive groups on each dendron should play an important role in surface reactivity and orientation. For example, the same concept has been used to manipulate the spacing between proteins, which has led onto the regulation of orientation and density of tethered proteins on surfaces (9). It will be interesting to examine whether ample spacing between the OEG chains affect intrinsic hydration of these layers and thus

* Corresponding author. E-mail: radvincula@uh.edu.
Received for review August 15, 2010 and accepted November 10, 2010
DOI: 10.1021/am100737s

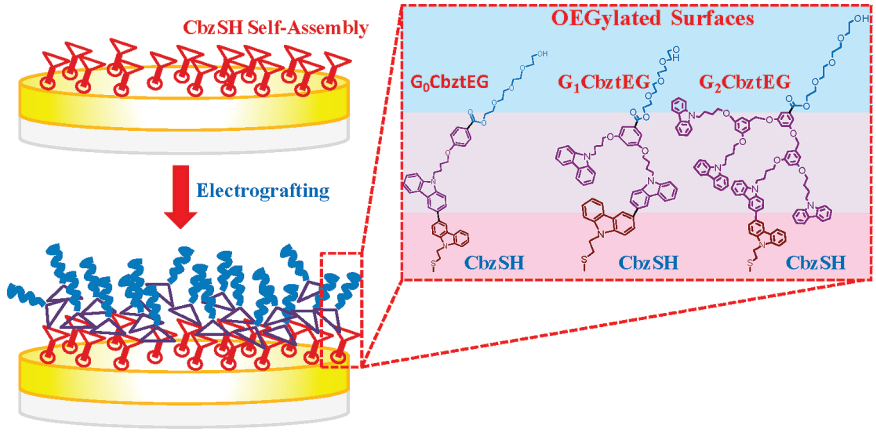

FIGURE 1. Target OEGylated linear carbazole dendron macromolecules.

surface protein resistance. Moreover, electrochemical reactivity implies that tethering can be done on most electrode surfaces (metal or metal oxides) by potentiostatic or potentiodynamic electrochemical methods, providing an alternative to the SAM approach. The overall objective then is to create biocompatible surfaces on various electrode surfaces suited for biomedical and sensing applications.

Three different generations of OEGylated carbazole dendrons, G_0CbztEG, G_1CbztEG, and G_2CbztEG, were synthesized. Their main structural features include: (a) dendronized carbazole moiety, which can be electrochemically polymerized on the surface and (b) peripheral hydroxyl groups for further chemical modification.

The synthesis of the target OEGylated ($n = 4$) carbazole dendrons was started by preparing the three different generations of carbazole-terminated dendrons utilizing a sonochemical Mitsonobu type etherification method as previously reported in our group (see the Supporting Information, Schemes 1−3) (10). Sonochemistry utilizes the chemical effects of ultrasound derive from acoustic cavitation—the formation, growth, and implosion of bubbles in a liquid irradiated with ultrasound (11). The sonication-mediated synthesis has reduced the reaction time from weeks or days to a couple of hours. The benzyl ether Frechet dendrons are synthesized in a facile convergent and stepwise manner resulting in an increase in carbazole peripheral functionality (exponentially). Initially, Frechet-type carbazole dendrons with methyl ester functionality were synthesized. Hydrolysis of the ester group yielded the corresponding acid for each generation (12). The substituted acid was coupled with tetraethylene glycol via dicyclohexylcarbodiimide coupling to afford the target OEGylated dendrons, G_0CbztEG, G_1CbztEG, and G_2CbztEG (Figure 1). ^{1}H NMR confirmed the structures of the desired OEGylated carbazole dendrons. The characteristic peaks found at 3.7−3.3 ppm are assigned to the addition of the ethylene glycol (OEG) units to the carbazole dendrons. The peaks assigned to OEG units were consistent with reported values in the literature (13−15). MALDI-TOF (matrix-assisted laser desorption ionization−time-of-flight) mass spectral analysis further confirmed the structures of the OEGylated linear-dendron molecules giving molecular ion peaks of 535.6007, 772.744, and 1458.9100 corresponding to G_0-, G_1-, and G_2-CbztEG.

As has been previously studied, carbazole is easily polymerized by cyclic voltammetry at low potential, resulting in polycarbazole linkages (16−18). Electrochemical grafting of these linear-dendrons onto conducting surfaces from a very dilute solution should allow for a very thin film of OEGylated molecules, provided that both the solvent and the potential (scan rate) are properly selected (19). The electrografting of acrylic end-capped PEG macromonomers was first reported by Jerome (19) and was found to be very efficient in preventing the adsorption of proteins. In our study, the OEGylated carbazole monodendrons were deposited on a modified Au substrate or indium tin oxide (ITO) by CV. By doing the deposition on thin Au (45 nm), this allowed us to directly study protein adsorption using surface plasmon resonance (SPR) spectroscopy. To facilitate improved adhesion, the Au substrates were modified by a thiol carbazole SAM using 5 mM solution at room temperature for 18 h. The CV deposition of 1 μM each of the G_nCbztEG dissolved in HPLC grade acetonitrile (0.01% max. water) was performed in a three-electrode cell containing 0.1 M tetrabutylammonium hexafluorophosphate as the supporting electrolyte. The electropolymerization was performed in each case by sweeping the voltage at a scan rate of 50 mV/s from 0 to 1.1 V against Ag/AgCl as a reference electrode and Pt as a counter electrode. Electrodeposition of the films was done in 20 cycles. These parameters were deemed to be optimum at this point and were used uniformly on the three molecules to facilitate comparison.

From the cyclic voltammogram (Figure 2a, c, e), the strong peak at 0.84−0.86 V (vs Ag/AgCl) for all the generations is due to the oxidation of the polycarbazole (12, 16−18). The CV diagrams gives a clear evidence of the electrografting behavior of the carbazole units. This represents the generation of radical cation species that lead to coupling of carbazoles at the 3,6-position and subsequent oligomerization (see the Supporting Information, Figure 6). The redox process is quasi-reversible for all the generations, giving a corresponding reduction peak at 0.78 − 0.80 V (vs Ag/AgCl). A shift toward lower oxidation peak with increasing number of cycles was also shown. Further, it can be observed that as the polymerization proceeds for each of the generations, the peak current increases in the successive cycles for all three molecules. For all three generations, the peak current

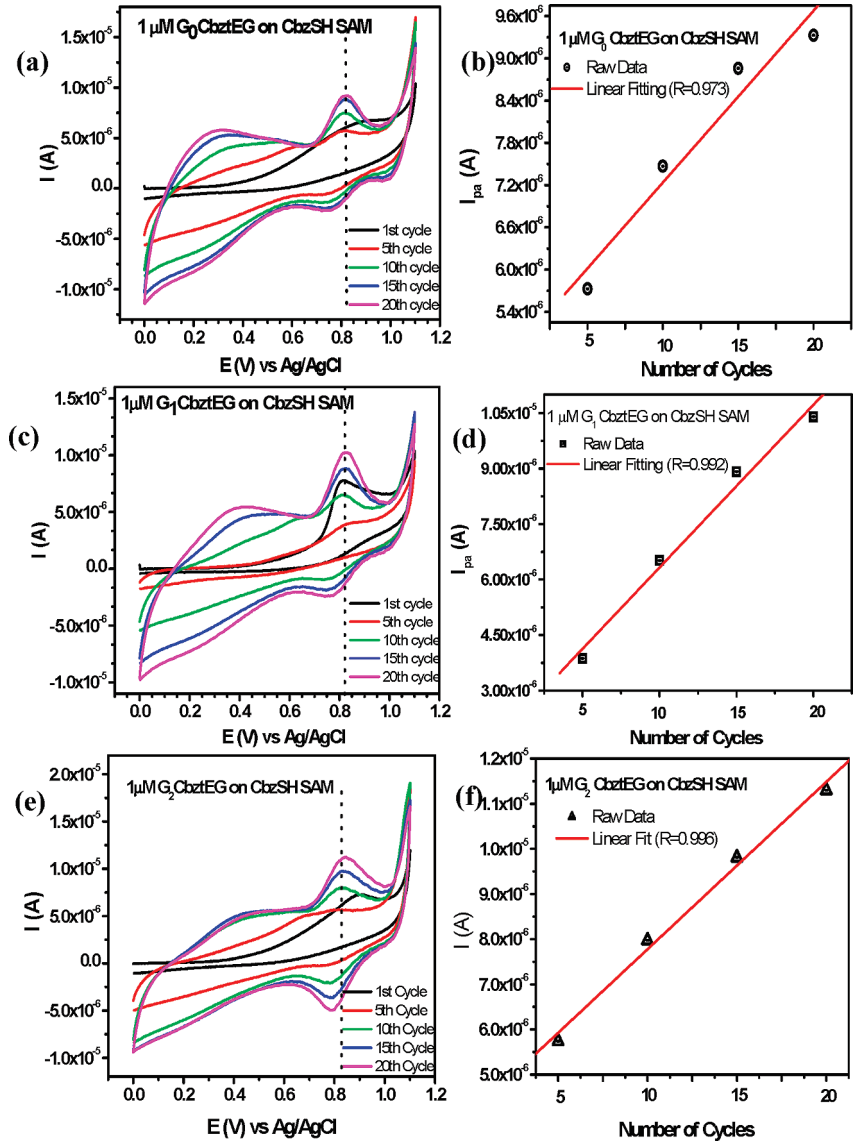

FIGURE 2. CV electropolymerization onto CbzSH SAM: (a) G_0CbztEG, (c) G_1CbztEG, and (e) G_2CbztEG. Plot of oxidation peak current (taken from the dotted line in the CV diagram) versus number of cycles during electrodeposition of (b) G_0CbztEG, (d) G_1CbztEG, and (f) G_2CbztEG onto CbzSH SAM.

demonstrates a linear increase with increasing number of CV cycles corresponding to the growth of the film (Figure 1b, d, f). Further evidence about the regular growth of the film via electropolymerization is verified in the SPR kinetic measurements (see the Supporting Information, Figure 2) illustrating a linear increase (correlation coefficient, $R \approx 0.99$) in the SPR angle for the entire growth of the film on Au substrate. This indicates that the growth of the polymer film on the electrode is very uniform (10).

Water contact angle measurements (see thhe Supporting Information, Table 1) showed a significant decrease in static contact angle for all the generations as compared to the water contact angle of the thiol carbazole SAMs. The decrease in water contact angle reflects the hydrophilic nature imparted by the OEG chains and therefore indicates the successful electrografting of the OEGylated carbazole dendrons on the electrodes. These contact angle measurements values were comparable with those measured by Bartz, et al. on the gold-coated glass slides after adsorption with the monothiol derived from tetraethylene glycol (13).

The ellipsometric thickness obtained for G_0-, G_1-, and G_2-CbztEG are 0.9, 1.4, and 2.8 ± 0.1 nm, respectively, suggesting the possible formation of a two-dimensionally (2-D) disordered but interconnected network polymer film. The AFM images revealed a good coverage and homogeneity of the films for all three generations as shown in the topography measurements (see the Supporting Information, Figure 3). Unlike an ideally pack SAM monolayer, the intra- and interchain linking of the electrodeposited molecules determine the conformation and orientation of the OEG units within the assembly (see the Supporting Information, Figure 6). Because OEG units are connected differently with the different dendron generations, this study should provide a new insight in the molecular conformation of the OEG units on the surface.

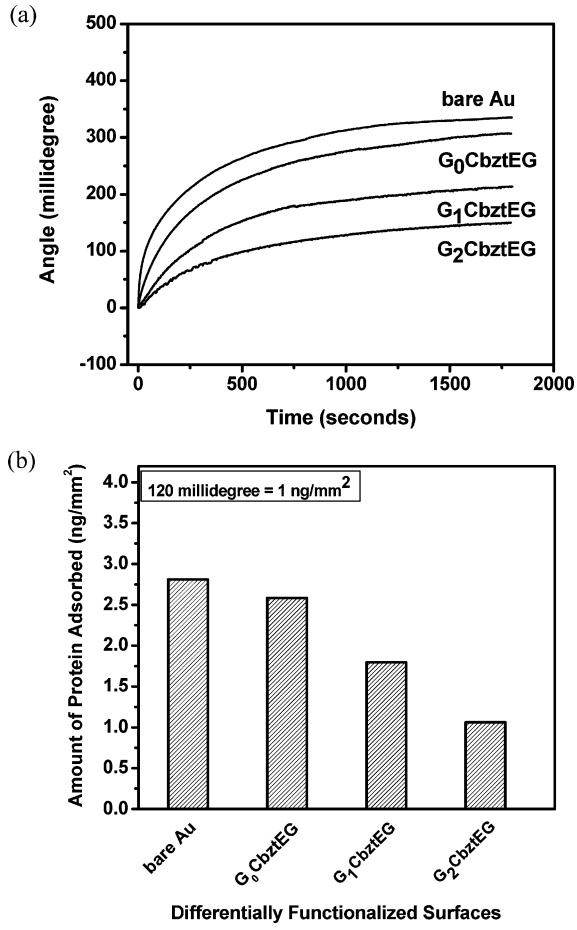

FIGURE 3. (a) SPR sensograms for 1 mg/mL Fb adsorption onto film prepared from G_0CbztEG, G_1CbztEG, and G_2CbztEG onto SHCbz-modified Au surfaces, and (b) amount of Fb adsorbed on differentially functionalized surfaces.

Nonspecific protein adhesion was evaluated by SPR spectroscopy. This technique allows for real-time and label-free detection of protein adsorption and its kinetics with high sensitivity (8). The choice of the model protein, fibrinogen (Fb), was prompted by the fact that this protein is one of the major constituents of human blood plasma and play a very important role in device rejection (20). Fb is a relatively big protein (340 kDa) which is negatively charged under the conducted experimental conditions. As shown in the SPR sensogram against fibrinogen (Figure 3), the film prepared from the highest generation G_2CbztEG monodendron showed the best protein-resistant film as compared to G_0CbztEG and G_1CbztEG. These data suggest that the dendron size dictates the orientation of the OEG chains available for intrinsic hydration that is responsible for protein repulsion. The possibility of greater intramolecular cross-linking in higher carbazole generations allows the coverage of a greater area of the substrate that probably hinders the collapse of the hydrophilic OEG moiety on the hydrophobic carbazole surface leading to a more protein-resistant film. It is also possible that this size of the anchoring dendron allows for the optimum distance between OEG units to allow a more native waterlike structure at the interface. This is in accordance to the observation of Whitesides et al. and Textor et al. that the decrease in chain mobility and hydration is the root cause of the loss of resistance at higher density (21, 22). Recently, Haag and co-workers (23) attributed the increase in the protein repelling property of films made from imperfect hyperbranched polyglycerol to the formation of "forestlike" monolayer, which gives the highest conformational freedom and therefore high mobility of the monolayer necessary to repel adsorption of proteins. Both of these factors may influence the G_2CbztEG to have the best protein resistant property from among the three generations. Studies are underway to compare the packing arrangement in a Langmuir–Blodgett film arrangement of the electropolymerized OEG-linear dendrons at the air–water interface.

Electrografting has the advantage of being applicable to a large variety of substrates, including metals and alloys, semiconductors, ITO-coated glass, and carbon (19). The CV traces of G_1CbztEG on three different substrates, ITO-coated glass, Au and doped Si, are shown in the Supporting Information (Figure 5). The oxidation peaks observed for these substrates at 0.83–1.1 V and the reduction peaks at 0.78–1.1 V correspond to the redox couples of the dicarbazyl species (16–18). The redox processes were also accompanied by the formation of a green colored film on the surface of the working electrode and the change from a pale yellow/colorless (reduced) into a green color (oxidized) solution, which are in good agreement with earlier reports (17, 18). The differences in CV are a consequence of the difference in electron transport kinetics between the conducting surfaces and perhaps the roughness. The electrodeposited film was further characterized by UV–vis spectroscopy. A peak with absorption maxima at about 396 nm was observed that corresponds to the π–π^* transitions attributed to the 3,3′-dicarbazyl radical cation (polaronic band or doped state) and the appearance of the broad peak in the 600–800 nm region confirming the highly conjugated nature of the materials deposited on the ITO substrates (12). AFM images (Figure 4) showed the deposition of globular shaped domain features of G_2CbztEG on ITO compared to the rough-edged surface of the native ITO substrate. This is comparable to some of the PEG and OEG grafted surfaces that have been examined by our group and others (24). The measured rms roughness is about 4 nm. Further studies are underway to investigate structure–property relationships on the thickness and morphology differentiation between the generations and their protein resistance properties.

In summary, three OEGylated carbazole monodendrons were synthesized and evaluated against fibrinogen. These linear-dendron molecules provide a novel method for introducing OEGylated materials on surfaces thru electrochemical grafting. Among the three generations of the carbazole monodendrons, the highest OEGylated carbazole generation, G_2CbztEG, showed the highest protein-resistant film which may be related to spacing and orientation of the OEG units on the surface. This study might provide an alternative system to SAM gold–thiol chemistry which can overcome some of the disadvantages but do not compromise the advantages of gold–thiol chemistry. New insights into the possible molecular mechanisms underlying OEGs protein

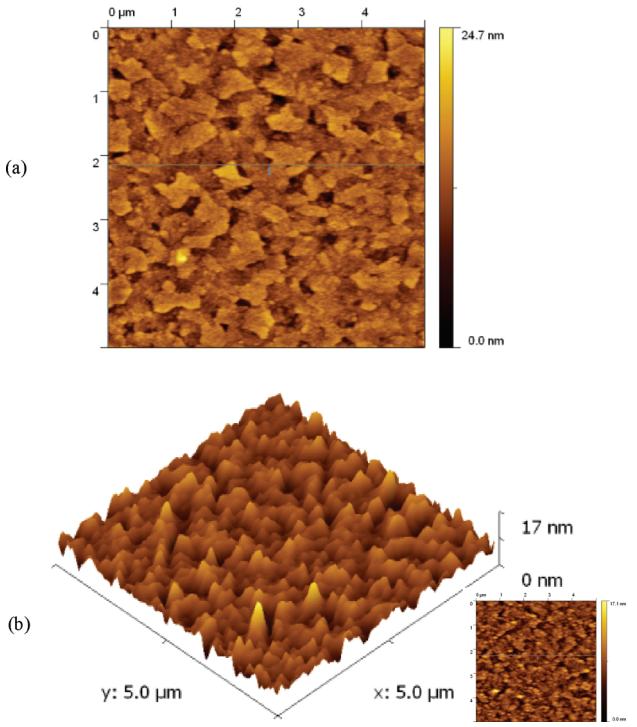

FIGURE 4. AFM images of (a) bare ITO, (b) topographic image of G_2CbztEG after CV deposition and 3D profile of the phase image of G_2CbztEG after CV deposition. The measure rms roughness is about 4 nm.

resistance should be possible. Monolayer LB film studies and their electropolymerization are underway.

Acknowledgment. The authors acknowledge funding from NSF DMR-10-06776, CBET-08-54979, CHE-10-41300, and Robert A. Welch Foundation, E-1551. Technical support from Metro Ohm, Agilent Technologies, and KSV Instruments (Biolin).

Supporting Information Available: Details of the syntheses and characterization data for all new compounds and additional electrochemical and film characterization data (PDF). This material is available free of charge via the Internet at http://pubs.acs.org.

REFERENCES AND NOTES

(1) Prime, K. L.; Whitesides, G. M. *Science* **1991**, *252*, 1164–1167.
(2) Senaratne, W.; Andruzzi, L.; Ober, C. K. *Biomacromolecules* **2005**, *6*, 2427–2448.
(3) Ratner, B. D. *J. Biomed Mater. Res.* **1993**, *27*, 837–850.
(4) Voccia, S.; Gabriel, S.; Serwas, H.; Jerome, J. *Prog. Org. Coat.* **2006**, *55*, 175–181.
(5) Elbert, D. L.; Hubbell, J. A. *Annu. Rev. Mater. Sci.* **1996**, *26*, 365–394.
(6) Grunze, M.; Harder, P.; Spencer, N. D.; Hahner, G.; Feldman, K. *J. Am. Chem. Soc.* **1999**, *121*, 10134–10141.
(7) Grunze, M.; Harder, P.; Dahint, R.; Whitesides, G. M.; Laibinis, P. E. *J. Phys. Chem. B* **1998**, *102*, 426–436.
(8) Li, L.; Chen, S.; Zheng, J.; Ratner, B.; Jiang, S. *J. Phys. Chem. B* **2005**, *109*, 2934–2941.
(9) Hong, B.; Jin, Oh, S.; Youn, T.; Kwon, S.l.; Park, J. *Langmuir* **2005**, *21*, 4257–4261.
(10) Taranekar, T.; Fulghum, T.; Patton, D.; Ponnapati, R.; Clyde, G.; Advincula, R. C. *J. Am. Chem. Soc.* **2007**, *129*, 12537–12548.
(11) Suslick, K. S.; Flannigan, D. J. *Annu. Rev. Phys. Chem.* **2008**, *59*, 659.
(12) Kaewtong, C.; Jiang, G.; Felipe, M. J.; Pulpoka, B.; Advincula, R. *ACS Nano* **2008**, *8*, 1533–1542.
(13) Bartz, M.; Kuther, J.; Nelles, G.; Weber, N.; Seshadri, R.; Tremel, W. *J. Mater. Chem.* **1999**, *9*, 1121–1125.
(14) Newkome, G. R.; Kotta, K.; Mishra, A.; Moorefield, C. N. *Macromolecules* **2004**, *37*, 8262–8268.
(15) Ding, L.; Chang, D.; Dai, L. *Macromolecules* **2005**, *38*, 9389–9392.
(16) Xia, C.; Advincula, R. C. *Chem. Mater.* **2001**, *13*, 1682–1691.
(17) Ambrose, J. F.; Nelson, R. F. R. *J. Electrochem. Soc.* **1968**, *115*, 1159–1164.
(18) Inzelt, G. *J. Solid-State Electrochem.* **2003**, *7*, 503–510.
(19) Gabriel, S.; Dubruel, P.; Schacht, E.; Jonas, A.; Gilbert, B.; Jerome, R.; Jerome, C. *Angew. Chem., Int. Ed.* **2005**, *44*, 5505–5509.
(20) Ratner, B. D.; Hoffman, A. S.; Schoen, F. J.; Lemons, J. E. *Biomaterials Science. An Introduction to Materials in Medicine*; Academic Press: San Diego, CA, 1996.
(21) Tosatti, S.; De Paul, S. M.; Askendal, A.; Vandevondele, S.; Hubbell, J. A.; Tengvall, P.; Textor, M. *Biomaterials* **2003**, *24*, 4949–4958.
(22) Harder, P.; Grunze, M.; Dahint, R.; Whitesides, G. M.; Laibinis, P. E. *J. Phys Chem. B* **1998**, *102*, 426–436.
(23) Haag, R.; Wyszogrodzka, M. *Langmuir* **2009**, *25*, 5703–5712.
(24) Sakellariou, G.; Park, M.; Advincula, R.; Mays, J. W.; Hadjichristidis, N. *J. Polym. Sci., Part A* **2006**, *44*, 769–782.

AM100737S